Envelope gating and noise shaping in populations of noisy neurons

J. W. Middleton,[1,2,3] E. Harvey-Girard,[2] L. Maler,[2,3] and A. Longtin[1,2,3]
[1]*Department of Physics, University of Ottawa, 150 Louis Pasteur, Ottawa, Canada K1N 6N5*
[2]*Department of Cellular and Molecular Medicine, University of Ottawa, 451 Smyth Road, Ottawa, Canada K1H 8M5*
[3]*Centre for Neural Dynamics, 451 Smyth Road, Ottawa, Canada K1H 8M5*
(Received 31 July 2006; published 28 February 2007)

Narrowband signals have fast and slow time scales. The transmission of narrowband signal features on both times cales, by spiking neurons, is demonstrated experimentally and theoretically. The interaction of the narrowband input and the threshold nonlinearity may create out-of-band interference, hindering the transmission of signals in a low-frequency range. The resultant out-of-band signal is the "envelope," or time-varying modulation of the narrowband signal. The levels of noise and nonlinearity intrinsic to the neuron gate transmission on the slow "envelope" time scale. When a narrowband and a distinct slow signal drive the neuron, the slow signal may be poorly transmitted. Increasing intrinsic noise in an averaging network removes the envelope in favor of the slow signal, paradoxically increasing the signal-to-noise ratio. These gating effects are generic for threshold and excitable systems.

DOI: 10.1103/PhysRevE.75.021918 PACS number(s): 87.19.La, 87.16.Xa, 87.19.Nn, 89.70.+c

Nonlinear dynamical systems driven by noise and harmonic signals can display a wide range of interesting phenomena. This is particularly the case for excitable and threshold systems in, e.g., laser physics and biology [1–4]. In physical systems, "harmonic" signals are often more of a narrowband nature, with power over a significant bandwidth (see Fig. 1). These have statistical properties intermediate to those of harmonic signals and broadband noise. Narrowband signals have at least two time scales: one related to a fast oscillation, or carrier, and a longer one related to the slow modulation, or envelope, of the carrier. Their effect has been studied in bistable systems [5,6], charge density waves in semiconductors [7] and in coupled Josephson junctions [8]. In the field of neuroscience, narrowband signals occur in natural stimuli [9–11]; they can, along with other signals, drive large-scale cortical activity [12,13]. A recent experimental study has further revealed that sensory systems can process the two time scales in parallel [11].

Rectification, which linearly transmits only one polarity of an analog signal, is known to be sufficient for extracting an envelope from a narrowband signal in physical systems [14,15]. How is this possible in noisy spiking neurons? How are the different time scales transmitted, and how does this interfere with transmission of other slow signals? These issues are the focus of this paper. We first demonstrate, using experiments and theory, how the neuron spiking threshold is key for generating a neural response at the envelope frequencies. In the aforementioned context of processing natural stimuli [9–11], this extraction is desirable, and noise is thus generally detrimental. Alternately, the envelope power may hamper the detection of other relevant low-frequency stimuli because their frequency bandwidths overlap with envelope bandwidths. This may arise, e.g., when a cortical cell participating in narrowband rhythmic activity generates envelope power and simultaneously tries to detect a low-frequency stimulus. In this context, envelope extraction from this narrowband activity is detrimental. We go on to show how a neuron population can overcome the "noisy background" caused by the extracted envelope. It can transmit low-frequency signals in the envelope bandwidth all the while responding coherently to the narrowband input. This enhancement of transmission, a new form of noise shaping, paradoxically arises from the addition of intrinsic uncorrelated noise in all neurons, with subsequent population averaging. This is in contrast to previous mechanisms involving reciprocal feedback in a network [16] or single cell negative interspike interval correlations [17]. Our results show how threshold nonlinearity and noise can gate the transmission of envelope power.

The model neuron used in this study is the leaky integrate-and-fire (LIF) neuron [18], with dynamics,

$$\frac{dv}{dt} = -\frac{v}{\tau} + I + \sqrt{\frac{2D}{\tau}}\xi(t) + S(t), \tag{1}$$

where v is the *trans*-membrane voltage, τ is the membrane

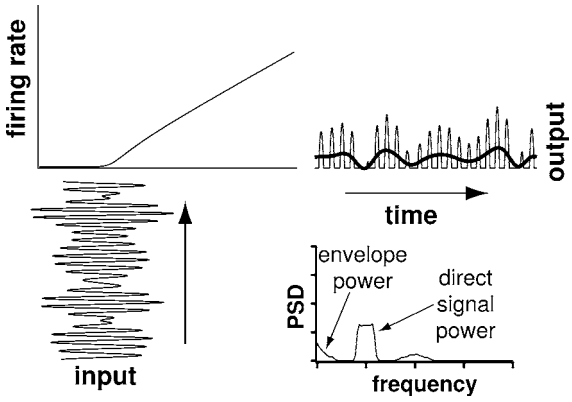

FIG. 1. A narrowband signal drives the input bias to a neuron near rheobase. The FI curve acts as a static transfer function, mapping the signal to a time-varying firing rate. Under these conditions, the output firing rate is a rectified version of the input (upper right). Also, the spectral power of this rate (bottom right) contains the same narrowband frequencies as the input, as well as the low frequencies of the slow time-varying envelope of this input. This envelope is seen here using a running average of the output rate over the fast time scale (thick line, upper right-hand panel).

time constant, I is the stationary input bias, and $S(t)$ is an input signal. The intrinsic membrane noise, $\xi(t)$, is a Gaussian white noise process, i.e., $\langle \xi(t)\xi(t')\rangle = \delta(t-t')$, with intensity D. This dynamics is supplemented with absorbing and reset boundaries at v_T and v_R, respectively. The times at which the voltage process is absorbed and reset represent spike times. The output spike train response $R(t)$ is represented by a sequence of Dirac delta functions at these times. For all following results, $S(t)$ is a narrowband Gaussian process with power in the 40–60 Hz range, and $E(t)$ is its low-frequency, time varying envelope. For comparison of the signal envelope $E(t)$ with the response $R(t)$, we need a nonlinear transformation to compute $E(t)$. This is done by taking the time-varying amplitude of the analytic signal via the Hilbert transform [19] which, in this case, yields an envelope signal with power in the 0–20 Hz range. The stationary mean rate of firing for the noisy LIF is given by [20]

$$r_0 = \left(\tau\sqrt{\pi} \int_{-(v_T - I\tau)/\sqrt{2D\tau}}^{-(v_R - I\tau)/\sqrt{2D\tau}} dz e^{z^2} \operatorname{erfc}(z) \right). \tag{2}$$

Below we will need the stationary rate as a function of input bias, $r_0(I)$, also known as the frequency-input (FI) curve.

In general, the nonlinear transfer function of any system has the ability to output low-frequency power associated with low-frequency modulations of a high-frequency carrier input [14,15]. The role of the FI curve as a sufficient nonlinearity to produce low-frequency envelope power in neural output is illustrated in Fig. 1. If a narrowband, time-varying input has its mean centered near rheobase (the input bias at which the neuron begins firing), the output firing rate will be a rectified version of the input, with slower dc offsets proportional to the time-varying envelope (Fig. 1, thick line, upper right-hand panel). The bottom right-hand panel of Fig. 1 shows the output represented in the frequency domain, with power in the bandwidth of the input signal as well as power in the lower frequency range associated with the slower time scale of the envelope.

The results of Fig. 1 suggest that the FI curve is a good approximate descriptor of the input-output transfer function of the neuron. This is particularly true in the context where the output firing rate tracks the input signal, i.e., rate-coding occurs. Henceforth, we refer to this descriptor as the "rate transfer model." This is also the primary ansatz of linear response theory in spiking neural models [21,22]. Except for comparison with experiments, this model will be kept in nondimensionalized form, apart for the time constant, $\tau = 10$ ms, which falls in the range of experimentally measured membrane time constants, and sets the firing frequency scale.

The measure of linear signal transfer we use between the input signal, $S(t)$, and the response, $R(t)$, is the frequency-dependent coherence, $C_{SR}(f) = |S_{SR}(f)|^2/[S_{SS}(f)S_{RR}(f)]$. $S_{SR}(f)$ is the cross-spectral density between the signal and the spike train response, and $S_{SS}(f)$ and $S_{RR}(f)$ are the autospectral densities of the signal and response, respectively. The coherence function can obtain values between 0 and 1.

The rate transfer model predicts that the response is more coherent with the envelope (i.e., a higher C_{ER}) when the average bias is near the rheobase [i.e., near $I=0.1$ in Eq. (1)].

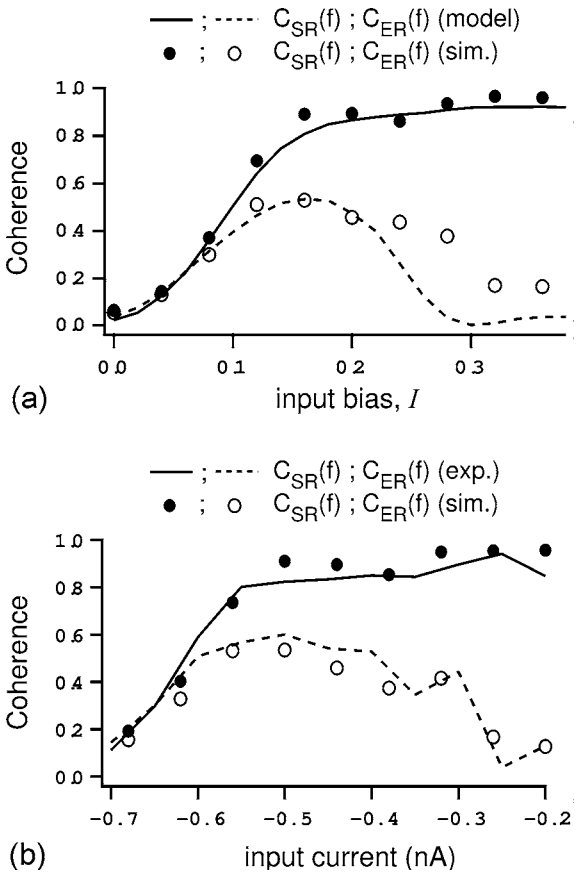

FIG. 2. (a) Comparison of coherences predicted by the rate transfer model [Eq. (2)] and by numerical simulation of Eq. (1). The solid line and filled circles show the coherence between a 40–60 Hz Gaussian signal and the output spike trains (SR coherence), as a function of input bias; the coherence is averaged over 40–60 Hz for each bias. The dashed line and open circles show coherence between the envelope of the same signal and the spike trains (ER coherence), averaged over the 0–20 Hz range of the envelope power. The noise intensity used is $D=5\times10^{-4}$. (b) Comparison of coherences between a 40–60 Hz Gaussian signal and the output spike trains of pyramidal cells *in vitro* and of simulated LIF neurons using Eq. (1) with the same parameters used in (a). Preparation of ELL slices and electrophysiology techniques were as in Ref. [23]. Experimental protocols were approved by the University of Ottawa Animal Care Committee.

Paradoxically, this enhanced linear coherence is a result of the threshold nonlinearity. We now wish to compare the output from Eq. (2) to the output from simulated neurons using Eq. (1). The I in Eq. (2) is replaced by $I+aS(t)$, where a is a frequency-independent scaling parameter fitted to match model FI and coherence to those of the simulated neuron. This simple scaling, akin to an average susceptibility over the input bandwidth, is sufficient here instead of the frequency-dependent susceptibility [22], provided that the stimulus bandwidth is narrow enough.

Figure 2(a) compares $C_{SR}(f)$ and $C_{ER}(f)$ calculated from the firing rate model (filled and open circles, respectively) and from numerical simulations of the LIF neuron (solid and dashed lines, respectively). For the rate transfer function model, two free parameters were used to account for the

background noise power in the 0–20 Hz and 40–60 Hz bandwidths expected for spike trains from a spontaneously firing neuron. These parameters were added to the output power of the rate transfer model in those bandwidths. $C_{SR}(f)$ increases with input bias and saturates for input biases corresponding to very high firing rates as a consequence of the general dependence of information transfer on firing rate [24]. $C_{ER}(f)$ increases with bias near the rheobase ($I=0.1$), but decreases for higher biases where the FI curve is more linear.

Next, we show that, qualitatively, the same dependence of $C_{SR}(f)$ and $C_{ER}(f)$ on input bias occurs in real neurons. Figure 2(b) compares a numerical simulation of the LIF model neuron and an *in vitro* recording made from a sample pyramidal cell. The input bias range for the model neuron was shifted and rescaled in units of (nA) to match firing rates for the range of injected currents (not shown). This same qualitative result was found in a total of $N=9$ cells. It has been previously shown that LIF neuron models can effectively reproduce first order firing statistics of real neurons, and also good qualitative fit to second order statistics with parameters fit to first order statistics [25]. We also find good agreement between real and simulated neurons using coherence as a higher order statistic. The real neurons show the predicted dependence of coherence on input current-saturation of $C_{SR}(f)$, and a nonmonotonic dependence for $C_{ER}(f)$. Higher input currents bring on a more linear regime and thus $C_{ER}(f)$ drops. Together, these results confirm the validity of the rate transfer model in describing the response of LIF neurons or real neurons to narrowband signals, and highlights the differences in the dependencies of $C_{SR}(f)$ and $C_{ER}(f)$ on bias.

The previous results were obtained in scenarios with relatively low levels of intrinsic noise. By and large, intrinsic membrane noise has a deleterious effect on the extraction and transmission of the signal envelope. Figure 3(a) shows the average $C_{ER}(f)$ as a function of mean input current from the rate transfer model for different values of noise intensity, D. The peak of $C_{ER}(f)$ decreases at least threefold as the noise increases over three orders of magnitude. The main effect of intrinsic noise is to wash out (i.e., linearize) the effective current threshold responsible for rectifying the input signal [20].

Figure 3(b) shows the effect of intrinsic noise on the power spectrum of a simulated spike train from a single neuron [Eq. (1)]. When intrinsic membrane noise is increased from $D=0.005$ to $D=0.5$ the entire broadband spectrum increases. The shape of the power spectrum is changed as well: the narrowband power at envelope frequencies (0–20 Hz) and higher harmonics of the fundamental frequency range are washed out relative to the background. We may then ask: *What effect does this noise-dependent spectral shaping have on signal transmission in neurons driven by narrowband rhythms?* In particular, since more noise washes out the power at envelope frequencies (relative to the background), can the system now better detect additional signals at these envelope frequencies—especially given that the total background noise power increases? The answer is relevant to neurons in different cortical areas that are subject to large spatial scale narrowband rhythms; these rhythms do not correspond to sensory stimuli but are often related to other tasks such as directing attention [12,13,26]. In this scenario, low-frequency envelope power would interfere with other signals being transmitted in the same envelope bandwidth. The addition of noise to a single cell removes the envelope power by linearizing the FI curve, but in doing so adds extra broadband power [Fig. 3(b)].

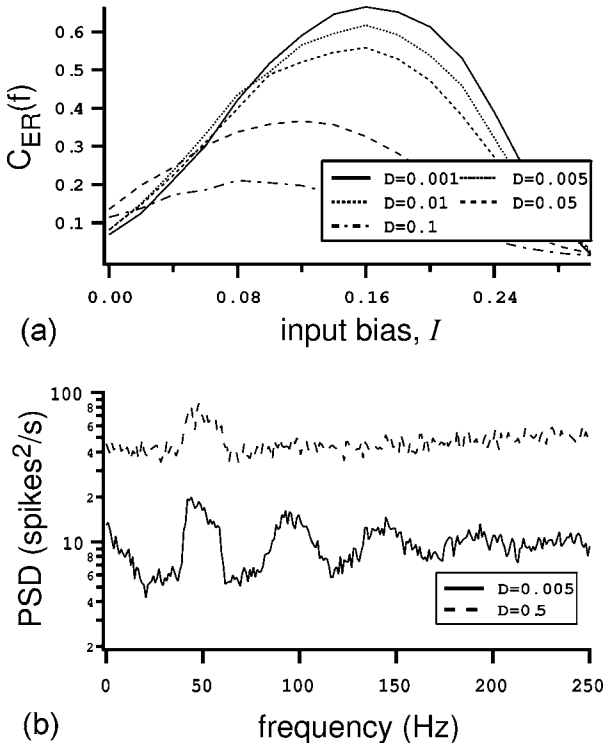

FIG. 3. The effects of noise intensity D in Eq. (1) on spike train envelope power. (a) The averaged values of $C_{ER}(f)$ as a function of input current, for different values of D in the rate transfer model of Eq. (2). (b) Ensemble averaged power spectra of the spike train of a simulated neuron, Eq. (1) with 40–60 Hz Gaussian input for a low and a high noise intensity, with $I=0.1$ and $\tau=10$ ms.

A solution to this problem involves averaging as follows. If the spike trains from a population of N identical neurons with independent intrinsic noises are averaged, the extra broadband power can be reduced as it varies as $1/N$. Figure 4(a) (inset, dashed, $D=0.5$) shows the power spectrum of the average spike train in a population of $N=50$ simulated neurons, displaying reduced envelope power relative to the power in the narrowband range (40–60 Hz). In the low noise case, the envelope component, common to all neurons, cannot be effectively averaged out [Fig. 4(a), inset, solid, $D=0.005$], unlike the intrinsic white noise, independent between all neurons. The arrows in Fig. 4(a) indicate the background noise levels ("noise floor") on top of which harmonic signal power is transmitted. This form of noise shaping differs from simply averaging out deleterious noise: it relies on a noise-mediated linearization of the signal transfer. The envelope signal, common to all neurons, is removed by the linearization and *then* the additional linearizing noise is averaged out. Thus noise may act as a gate of linear vs nonlinear information in the brain.

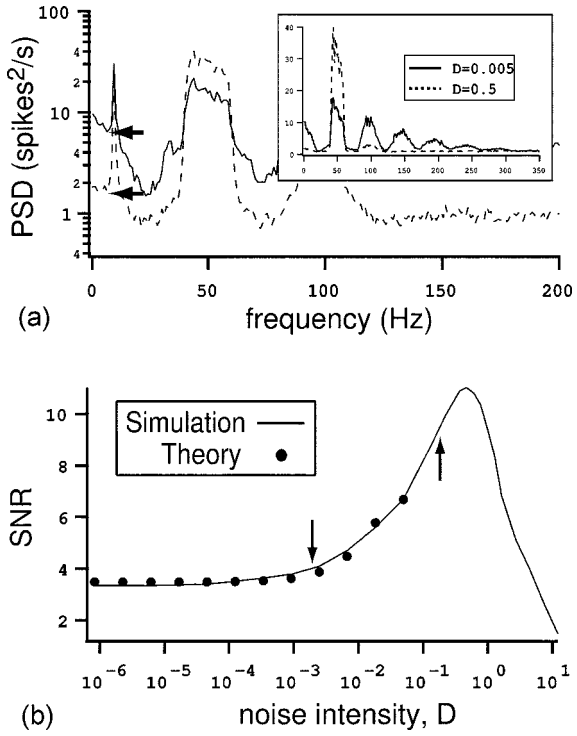

FIG. 4. Network averaging of spike trains $R(t)=\Sigma_{j=1}^{N}R_j(t)/N$ from independent noisy neurons shapes the average spike train power spectrum. (a) The power spectral density of the average spike train $R(t)$ with $N=50$ identical LIF neurons with independent uncorrelated noise for $D=0.005$ (dashed line) and $D=0.5$ (solid line). The noise floor (indicated by arrows) is paradoxically reduced with the addition of intrinsic noise, so that the power of a small amplitude, low-frequency ($f=10$) harmonic input is more visible. The inset shows the effect of noise on the full spectrum in the absence of a low-frequency, harmonic input. (b) The SNR of the averaged spike train $R(t)$ with respect to this low-frequency harmonic input shows a nonmonotonic behavior as a function D (solid line). A noise-dependent rheobase shift predicts the behavior of the SNR for low to moderate noise intensities (circles). The arrows indicate the SNR for noise values used in (a).

Figure 4(b) shows the effects of this form of noise shaping (noise floor changes) on low-frequency signal transmission. When the small amplitude sinusoidal input [shown in Fig. 4(a)], with frequency f_o in the envelope bandwidth, is added, the signal-to-noise ratio $\{\mathrm{SNR}=\lim_{\epsilon\to 0} 2S(f_o)/[S(f_o-\epsilon)+S(f_o+\epsilon)]\}$ depends on D. The SNR with respect to this harmonic signal increases with D up to a point, and then decreases when the single cells can no longer respond coherently in the presence of high noise. The increase in SNR can be modeled by considering that the envelope power is extracted from rectification by the FI rate transfer model in Eq. (2). A general, biased rectifying device results in total envelope power proportional to A^2-B^2 where A^2 is the signal variance and B is the rectifying bias [14], which is the difference between the mean of the input signal, I, and the threshold ($B=0$ thus corresponding to half-wave rectification). Increasing noise has the effect of shifting the threshold (rheobase in our case) leftwards.

With this in mind, we can make a first-order approximation that increasing the noise shifts the rectifying bias, i.e., $B\propto k-D$ where k is an arbitrary constant. A small noise expansion of the SNR gives a second-order polynomial, $\mathrm{SNR}\approx a-bD+cD^2$. The resulting formula was fit (circles) to the numerical simulation results (solid lines) in Fig. 4(b), thereby showing that a noise-induced rheobase shift is responsible for the low to moderate noise behavior of the SNR in our averaging network. Even though classic stochastic resonance (SR, i.e., the matching of noise induced threshold crossing times with stimulus period) is possible in this model neuron, namely for very low mean input bias [see Fig. 3(a)], it does not play a role in this noise shaping, since the bias I used for Figs. 3 and 4 is not subthreshold. This effect also differs from superthreshold stochastic resonance (SSR) [27]. In SSR the addition of noise increases the SNR by increasing the effective sampling rate of a high-frequency signal. Here we remove extra "background" low-frequency power, by linearizing and then averaging, thus increasing SNR.

In summary, we have examined the nature of envelope extraction in biophysical spiking neurons and confirmed the validity of the underlying mechanism in pyramidal cell recordings *in vitro*. The envelope-response coherence, $C_{\mathrm{ER}}(f)$, shows a strong dependence on average current inputs as well as on intrinsic membrane noise. This mechanism could play a role in gating the flow of envelope information in sensory systems where the envelope represents a pertinent cue [9,10,28]. Also, our results lead us to hypothesize that a form of noise shaping can occur which enables gating of different kinds of information through the same physical channel (i.e., single neurons), depending on the context. This can take place, e.g., in cortical areas, where macroscopic rhythms [11–13,26] and neurons with high degrees of variability [29] are found. This noise shaping is mediated by an increase in intrinsic noise as opposed to network connectivity [16] or intrinsic single cell temporal correlations [17]. Experimental validation of this hypothesis may be difficult *in vivo*, although we predict this noise shaping could be observed in iterated network experiments [30] *in vivo*. The envelope response described here is a generic property of a single threshold and/or excitable system; this further implies that this form of noise shaping will be a generic property of arrays of such systems.

Funding was provided by NSERC, OGSST, and CIHR. The authors thank B. Doiron and M. J. Chacron for useful discussions.

[1] B. Lindner, J. Garcia-Ojalvo, A. Neiman, and L. Schimansky-Geier, Phys. Rep. **392**, 321 (2004).
[2] L. Gammaitoni, P. Hanggi, P. Jung, and F. Marchesoni, Rev. Mod. Phys. **70**, 223 (1998).
[3] P. Jung, Phys. Rep. **234**, 175 (1993).
[4] C. S. Zhou, J. Kurths, E. Allaria, S. Boccaletti, R. Meucci, and F. T. Arrechi, Phys. Rev. E **67**, 015205 (2003).
[5] M. I. Dykman, R. Mannella, P. V. E. McClintock, N. D. Stein, and N. G. Stocks, Phys. Rev. E **47**, 3996 (1993).
[6] A. Neiman and L. Schimansky-Geier, Phys. Rev. Lett. **72**, 2988 (1994).
[7] M. S. Sherwin and A. Zettl, Phys. Rev. B **32**, 5536 (1985).
[8] M. E. Inchiosa, V. In, A. R. Bulsara, K. Wiesenfeld, T. Heath, and M. H. Choi, Phys. Rev. E **63**, 066114 (2001).
[9] J. C. L. Baker and I. Mareschal, J. Clim. **134**, 171 (2001).
[10] L. Liang, T. Lu, and X. Wang, J. Neurophysiol. **87**, 2237 (2002).
[11] J. W. Middleton, J. Benda, A. Longtin, and L. Maler, Proc. Natl. Acad. Sci. U.S.A. **103**, 14596 (2006).
[12] V. V. Nikouline, K. Linkenkaer-Hansen, J. Huttunen, and R. J. Ilmoniemi, NeuroReport **12**, 2487 (2001).
[13] G. Buzsáki and A. Draguhn, Science **304**, 1926 (2004).
[14] S. O. Rice, in *Selected Papers on Noise and Stochastic Processes*, edited by N. Wax (Dover, New York, 1954).
[15] D. Middleton, *An Introduction to Statistical Communication Theory* (McGraw-Hill, New York, 1960).
[16] D. J. Mar, C. C. Chow, W. Gerstner, R. W. Adams, and J. J. Collins, Proc. Natl. Acad. Sci. U.S.A. **96**, 10450 (1999).
[17] M. J. Chacron, B. Lindner, and A. Longtin, Phys. Rev. Lett. **92**, 080601 (2004).
[18] L. Lapique, J. Physiol. Pathol. Gen. **9**, 620 (1907).
[19] A. V. Oppenheim and R. W. Schafer, *Discrete Time Signal Processing* (Prentice Hall, Upper Saddle River, NJ, 1999).
[20] H. C. Tuckwell, *Introduction to Theoretical Nurobiology* (Cambridge University Press, Cambridge, 1988).
[21] N. Fourcaud and N. Brunel, Neural Comput. **14**, 2057 (2002).
[22] B. Lindner and L. Schimansky-Geier, Phys. Rev. Lett. **86**, 2934 (2001).
[23] N. J. Berman and L. Maler, J. Neurophysiol. **80**, 3214 (1998).
[24] A. Borst and J. Haag, J. Comput. Neurosci. **10**, 213 (2001).
[25] A. Rauch, G. L. Camera, H. R. Luscher, W. Senn, and S. Fusi, J. Neurophysiol. **90**, 1598 (2003).
[26] T. Womelsdorf, P. Fries, P. P. Mitra, and R. Desimone, Nature **439**, 7077 (2006).
[27] N. G. Stocks, Phys. Rev. Lett. **84**, 2310 (2000).
[28] J. F. Schouten, R. J. Ritsma, and B. L. Cardozo, J. Acoust. Soc. Am. **34**, 1418 (1962).
[29] M. N. Shadlen and N. W. T. Newsome, J. Neurosci. **18**, 3870 (1998).
[30] A. D. Reyes, Nat. Neurosci. **6**, 593 (2003).